Histometabolic tumor imaging of hypoxia in oral cancer: clinicopathological correlation for prediction of an aggressive phenotype

Morand, G B ; Broglie, Martina A ; Schumann, Paul ; Hüllner, Martin W ; Rupp, Niels J

Abstract: Introduction: Fluorodeoxyglucose-positron emission tomography (FDG-PET) is a widely used imaging tool for oral squamous cell carcinoma (OSCC). Preliminary studies indicate that quantification of tumor metabolic uptake may correlate with tumor hypoxia and aggressive phenotypes. Methods: Retrospective review of a consecutive cohort of OSCC (n = 98) with available pretherapeutic FDG-PET/CT, treated at the University Hospital Zurich. Clinico-pathologico-radiological correlation between maximum standard uptake value (SUVmax) of the primary tumor, immunohistochemical staining for hypoxia-related proteins glucose transporter 1 (GLUT1) and hypoxia-inducible factor 1-alpha (HIF1a), depth of invasion (DOI), lymph node metastasis, and outcome was examined. Results: Positive staining for GLUT1 and HIF1a on immunohistopathological analysis correlated with increased SUVmax on pretherapeutic imaging and with increased DOI (Kruskal–Wallis, P = 0.037, and P = 0.008, respectively). SUVmax and DOI showed a strong positive correlation (Spearman Rho, correlation coefficient = 0.451, P = 0.0003). An increase in SUVmax predicted nodal metastasis (Kruskal–Wallis, P = 0.017) and poor local control (log rank, P = 0.047). Conclusion: In OSCC, FDG-PET-derived metabolic tumor parameter SUVmax serves as a surrogate marker for hypoxia and can be used to predict tumor aggressiveness, with more invasive phenotypes and poorer local control.

DOI: https://doi.org/10.3389/fonc.2020.01670

frontiers in Oncology

ORIGINAL RESEARCH
published: 27 August 2020
doi: 10.3389/fonc.2020.01670

Histometabolic Tumor Imaging of Hypoxia in Oral Cancer: Clinicopathological Correlation for Prediction of an Aggressive Phenotype

Grégoire B. Morand[1,2], Martina A. Broglie[1,2], Paul Schumann[2,3], Martin W. Huellner[2,4] and Niels J. Rupp[2,5]*

[1] Department of Otorhinolaryngology, Head and Neck Surgery, University Hospital Zurich, Zurich, Switzerland, [2] Faculty of Medicine, University of Zurich, Zurich, Switzerland, [3] Department of Cranio-Maxillo-Facial and Oral Surgery, University Hospital Zurich, Zurich, Switzerland, [4] Department of Nuclear Medicine, University Hospital Zurich, Zurich, Switzerland, [5] Department of Pathology and Molecular Pathology, University Hospital Zurich, Zurich, Switzerland

OPEN ACCESS

Edited by:
Dietmar Thurnher,
Medical University of Graz, Austria

Reviewed by:
Einar Dale,
Consultant, Oslo, Norway
Cesare Piazza,
Istituto Nazionale dei Tumori (IRCCS), Italy

***Correspondence:**
Grégoire B. Morand
gregoire.morand@usz.ch;
gregoire.morand@mail.mcgill.ca

Specialty section:
This article was submitted to Head and Neck Cancer, a section of the journal Frontiers in Oncology

Received: 13 April 2020
Accepted: 28 July 2020
Published: 27 August 2020

Citation:
Morand GB, Broglie MA, Schumann P, Huellner MW and Rupp NJ (2020) Histometabolic Tumor Imaging of Hypoxia in Oral Cancer: Clinicopathological Correlation for Prediction of an Aggressive Phenotype. Front. Oncol. 10:1670. doi: 10.3389/fonc.2020.01670

Introduction: Fluorodeoxyglucose-positron emission tomography (FDG-PET) is a widely used imaging tool for oral squamous cell carcinoma (OSCC). Preliminary studies indicate that quantification of tumor metabolic uptake may correlate with tumor hypoxia and aggressive phenotypes.

Methods: Retrospective review of a consecutive cohort of OSCC (n = 98) with available pretherapeutic FDG-PET/CT, treated at the University Hospital Zurich. Clinico-pathologico-radiological correlation between maximum standard uptake value (SUV_{max}) of the primary tumor, immunohistochemical staining for hypoxia-related proteins glucose transporter 1 (GLUT1) and hypoxia-inducible factor 1-alpha (HIF1a), depth of invasion (DOI), lymph node metastasis, and outcome was examined.

Results: Positive staining for GLUT1 and HIF1a on immunohistopathological analysis correlated with increased SUV_{max} on pretherapeutic imaging and with increased DOI (Kruskal–Wallis, P = 0.037, and P = 0.008, respectively). SUV_{max} and DOI showed a strong positive correlation (Spearman Rho, correlation coefficient = 0.451, P = 0.0003). An increase in SUV_{max} predicted nodal metastasis (Kruskal–Wallis, P = 0.017) and poor local control (log rank, P = 0.047).

Conclusion: In OSCC, FDG-PET-derived metabolic tumor parameter SUV_{max} serves as a surrogate marker for hypoxia and can be used to predict tumor aggressiveness, with more invasive phenotypes and poorer local control.

Keywords: carcinoma, squamous cell, fluorodeoxyglucose, tumor hypoxia, mouth neoplasms, positron emission tomography, glucose transporter type 1, lymph nodes

INTRODUCTION

Oral squamous cell carcinoma (OSCC) is an aggressive malignancy characterized by local invasiveness and high propensity for early nodal dissemination (1, 2). The importance of depth of invasion (DOI) of the primary tumor and its correlation with the prevalence of lymph node metastasis is now widely recognized. It was implemented into the latest edition of the tumor–node–metastasis (TNM) classification system (3, 4).

Oral squamous cell carcinoma undergoes phenotypic changes to gain migratory and invasive properties through the process of epithelial–mesenchymal transition (EMT) (5, 6). Enrichment in EMT sustains transcription of several matrix metalloproteinases, initiating focal matrix degradation and allowing invasion (7). EMT also enhances the glycolytic phenotype of cancer cells that are exposed to hypoxia (6). Tumor cells increasingly metabolize glucose through glycolysis rather than oxygen-dependent Krebs cycle when exposed to hypoxia. This phenomenon is often referred to as the Warburg effect (8).

Clinically, glucose consumption of tumors can be estimated pretherapeutically by functional nuclear medicine imaging with 18-fluoro-desoxy-glucose positron emission tomography (FDG-PET). Imaging metabolic parameters, such as maximum standard uptake value (SUV_{max}), provide *in vivo* quantification of the glucose consumption of a particular tumor (9–11).

As EMT, tumor hypoxia, and the Warburg effect are intricately related (12, 13), we postulated that immunohistochemical expression of hypoxia-related proteins correlates with higher glucose consumption and more invasive phenotype of OSCC. The prognostic relevance of hypoxia in oral cancer has already been reported by other studies before, mostly using immunohistochemical staining for hypoxia biomarker such as hypoxia-inducible factor 1-alpha (HIF1a) and glucose transporter 1 (GLUT1 or other proteins such as CD44) (14–17). However, very few studies have combined immunohistochemical and oncological outcome and functional imaging data in oral cancer (18–21). We therefore examined the role of hypoxia in OSCC comparing clinical, histological, and functional imaging data, therefore creating a histometabolic profile of OSCC. We also assessed its impact on local control and metastatic spread.

MATERIALS AND METHODS

Study Population

After ethical review board approval (protocol number 2016-01799, including amendment dated December 14th, 2018), the charts of consecutive histologically proven OSCC patients were retrospectively assessed. Patients treated from 2007 to 2018 at the Department of Otorhinolaryngology—Head and Neck Surgery, University Hospital Zurich, Switzerland, with available pretherapeutic FDG-PET [combined with computed tomography (CT) or magnetic resonance imaging (MRI)] were included. According to our institutional policy, all patients with primary tumors staged clinically as either $\geq$ cT3 or $\geq$ cN2b underwent pretherapeutic FDG-PET (11). Therefore, the study cohort included mainly patients with advanced OSCC stages. Only patients treated with curative intent and without distant metastasis at initial presentation were included. Patients with previous treatment of another head and neck squamous cell carcinoma and/or patients after induction chemotherapy were excluded. Adjuvant radio(chemo)therapy was administered according to the National Comprehensive Cancer Network (NCCN) guidelines after review of final pathology (22).

Detailed data on age, gender, smoking, drinking habits, clinical and pathological stage, DOI, number of lymph nodes dissected, number of positive lymph nodes, local and regional recurrence, distant metastasis, disease-specific survival, and overall survival were obtained. Patients were staged according to the *Union Internationale Contre le Cancer (UICC)*, TNM staging for head and neck cancer, 8th edition 2017 (3).

Immunohistochemistry and Immunohistochemical Scoring

An automated Ventana BenchMark Ultra (Roche-Ventana Medical System, Tucson, AZ, United States) was used for staining according to the manufacturer's instructions. Immunohistochemical staining for CD44, for GLUT1, and for HIF1a were performed according to previous studies by our group (4, 23). Positive and negative controls were included in all reactions. Immunohistochemical scoring assessing the whole histological slides was performed by a board-certified pathologist (NJR) and board-certified head and neck surgeon (GBM). For equivocal cases, a consent was reached. If necessary, hematoxylin, and eosin slides were assessed as well. NJR and GBM were blinded to the outcome and further clinicopathological data during the scoring.

CD44 and GLUT1 both showed a distinct membranous staining and were scored in a four-tiered system [negative, weak (1+), moderate (2+), and strong (3+) according to a previous publication (4)]. For GLUT1 (polyclonal antibody, 1:1,000, Millipore), staining of nearby erythrocytes was used as a positive control. HIF1a (antibody clone mgc3, 1:400, Abcam Limited) showed a nuclear staining and was scored with a similar system as GLUT1, ranging from 0 to 2+. A score of 1 + demonstrated at least 10% of tumor cells with nuclear staining.

The hypoxia score was created adding the GLUT1 score (0–3+) and the binarized HIF1a score, therefore ranging from 0 to 4+.

FDG-PET/CT or FDG-PET/MR Image Acquisition

All patients fasted for at least 4 h prior to the scan. Patients were injected with a standardized dose of 3.5 MBq FDG/kg body weight (analog PET/CT) or a body mass index (BMI)-adjusted FDG dosage protocol (digital PET/CT and PET/MR) (24). All patients had a blood glucose level below 10 mmol/L before imaging. During the uptake time of 1 h, patients rested in a silent, warm, and dimmed environment. Scans were acquired using integrated PET/CT scanners (Discovery VCT, Discovery 690, or Discovery MI, GE Healthcare, Waukesha, WI, United States) or an integrated PET/MR scanner (Signa PET/MR, GE Healthcare). Scans included either a diagnostic CT scan of the neck after

administration of iodinated contrast medium or a diagnostic regionalized PET/MR scan of the neck using gadolinium-based contrast medium. Detailed technical acquisition protocols have been published previously (11).

Metabolic Parameters

The standardized uptake value (SUV) was calculated automatically [activity in volume of interest (VOI)/(injected dose × body weight)]. The SUV_{max} is defined as the hottest voxel within the VOI. SUV_{mean} is defined as the average SUV of voxels within the VOI exceeding 42% of the SUV_{max}. The metabolic tumor volume (MTV) is defined as the sum of the volume of voxels with an SUV exceeding a threshold of 42% of the SUV_{max} within the VOI. Total lesion glycolysis (TLG) is defined mathematically as MTV × SUV_{mean}. For the analysis of FDG uptake, correct placement of volumes of interest on PET images is ensured by side-by-side reading of the corresponding CT or MR images. A written radiological report by a doubly board-certified nuclear medicine physician/radiologist was available for all FDG-PET/CT or FDG-PET/MR examinations.

Statistical Analysis

Mean, standard deviation (±SD), standard error of mean (±SEM), median, or interquartile range (IQR) are given for descriptive analysis of continuous variables. For comparison of means, the *t* test was used for normally distributed variables. Alternatively, the non-parametric Kruskal–Wallis test was used. Binary variables were associated in contingency tables using the chi-squared test.

For primary outcome analysis, correlations between continuous variables were assessed using the Spearman rho test. Curve estimations were performed using a linear model not including a constant in the equation. Receiver operating characteristic (ROC) curve was used to select the best cutoff value for SUV_{max} to predict DOI > 10 mm with the 95% confidence interval provided (95% CI). The relative sensitivity and specificity were calculated according to the Bayes' theorem. For secondary outcome analysis, survival curves were built according to Kaplan–Meier, and the log-rank test was used to compare factors. Finally, a Cox regression model was built to assess survival in multivariable analysis, including all relevant baseline characteristics (**Table 1**), the hypoxia score, and SUV_{max} of the primary tumor. We did not include DOI in the model because DOI is collinear with T-classification and with SUV_{max} of primary tumor. Inclusion of DOI leads to instability of the model (25). A $P \leq 0.05$ was considered to indicate statistical significance. Statistical analyses were performed using SPSS 25.0.0.1 software (IBM, Armonk, NY, United States).

RESULTS

Patient and Tumor Characteristics

A total of 98 consecutive patients were included in the study. The mean age at diagnosis was 65.4 (SD, 13.3) years. There was a clear male predominance with 64 (65.3%) male and 34 (34.7%) female patients. Forty-one (41.8%) had squamous cell carcinomas of the oral tongue, 32 (32.7%) of the floor of mouth, and 17 (17.3%) of the gum. Eight (8.2%) tumors were located elsewhere (retromolar trigone, buccal mucosa). Slightly more than half (56, 57.1%) of the patients had pT1–pT2 tumors, while 42 (42.9%) had pT3–pT4 tumors. All patients underwent pathological assessment of nodal status, 12 (12.2%) of these with sentinel lymph node biopsy, the remaining 86 (87.8%) with neck dissection. Of those, 12 (12.2%) had bilateral neck dissection. Mean number of dissected nodes for sentinel, unilateral, and bilateral neck dissection was 2.8 (±SEM 0.6), 25.8 (±SEM 1.2), and 48.4 (±SEM 4.1), respectively. Nodal status was positive (pN+) in 49 patients (50%), of which 16 (16.5%) were staged with pN1, 20 (20.4%) pN2a–pN2b, and 13 (13.2%) pN2c–pN3 categories (**Table 1**).

TABLE 1 | Baseline characteristics of study patients.

Variable	All patients No. = 98
Age (years)	
Mean (SD)	65.4 (SD 13.3)
Gender	
Male	64 (65.3%)
Female	34 (34.7%)
Smoking	
Yes	56 (55.4%)
No	45 (44.6%)
Alcohol	
Yes	40 (39.6%)
No	61 (60.4%)
Tumor subsite	
Oral tongue	41 (41.8%)
Floor of mouth	32 (32.7%)
Upper/lower gum	17 (17.3%)
Other	8 (8.2%)
T category	
pT1/pT2	56 (57.1%)
pT3/pT4	42 (42.9%)
N category	
pN0	49 (50.0%)
pN+	49 (50.0%)

No., number and SD, standard deviation.

In total, 59 (60.2%) patients received adjuvant radiotherapy with a mean local dose of 60.5 Gy (±SEM 1.2) and 52.3 Gy (±SEM 2.7) for the nodal basin. 20 (20.4%) patients received concomitant chemotherapy. Mean follow-up time of the cohort was 24.2 months (±SEM 2.1).

A High Primary Tumor SUV_{max} Correlates With Deep Invading Tumors

In a first step, we examined whether metabolic tumor imaging showed a correlation with histological DOI of the primary tumor. DOI and SUV_{max} showed a strong positive correlation (**Figure 1**, Spearman Rho, correlation coefficient = 0.451, and $P = 0.0003$). A similar observation could be made when correlating DOI and MTV (Spearman Rho, correlation coefficient = 0.486, $P = 0.004$, not shown). TLG did not correlate significantly with DOI ($P > 0.05$, not shown).

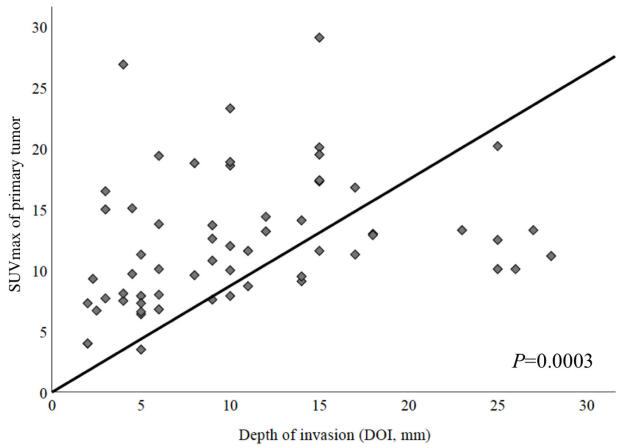

FIGURE 1 | Correlation between maximum standardized uptake value (SUV_{max}) of primary tumor and depth of invasion (DOI). These parameters showed a strong positive correlation (Spearman Rho, correlation coefficient = 0.451, P = 0.0003).

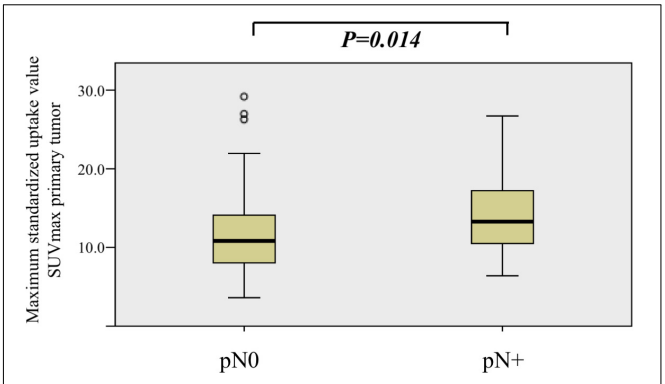

FIGURE 2 | Comparison of maximum standardized uptake value (SUV_{max}) value distribution among nodal positive (pN+) and nodal negative (pN0) patients. SUV_{max} was significantly higher in the nodal positive (pN+) group (Kruskal–Wallis test, P = 0.013).

Various cutoff values for SUV_{max} were tested. Using ROC curves, the best potential cutoff value for the pretherapeutic SUV_{max} of primary tumor was determined to be 9.5 for the highest sensitivity and 14.5 for the highest specificity, respectively, [area under the curve (AUC), 70.8% (95% CI, 57.8–83.8%); P = 0.007; **Table 2**].

A High Primary Tumor SUV_{max} Is Associated With Positive Neck Disease

Second, we compared the distributions of SUV_{max} of primary tumors among patients with positive and negative nodal disease (pN + vs. pN0).

The median SUV_{max} of primary tumor was 13.2 (IQR, 10.1–17.1) and 11.0 (IQR, 7.8–15.1) in the nodal positive and negative group, respectively.

When comparing the distribution of SUV_{max} among pN+ and pN0, there was a statistically significant difference between the two groups (Kruskal–Wallis test, P = 0.013, **Figure 2**).

TABLE 2 | Diagnostic accuracy of SUV_{max} in prediction of depth of invasion.

Variable	Depth of invasion < 10 mm		
SUVmax primary tumor < 9.5	TP	FP	Sensitivity
	21	19	87.5%
	FN	TN	Specificity
	3	17	47.2%
SUVmax primary tumor > 14.5	TP	FP	Sensitivity
	7	9	29.2%
	FN	TN	Specificity
	17	27	75.0%

SUV_{max}, standardized maximum uptake value; TP, true positive; FP, false positive; FN, false negative; and TN, true negative.

Correlation Between SUV_{max}, Immunohistochemical Surrogates for Hypoxia, and Depth of Invasion

Furthermore, we analyzed immunohistochemical stainings for the glucose transporter protein GLUT1 in primary tumor samples. Patients showing a strong expression of GLUT1 (score > 2+) had a significantly higher SUV_{max} (Kruskal–Wallis test, P = 0.028) than patients with low/moderate (score ≤ 2+) expression of GLUT1. For MTV and TLG, there was no statistical difference (Kruskal–Wallis test, P = 0.107 and P = 0.160), respectively. Strong expression of GLUT1 was also associated with greater DOI (Kruskal–Wallis test, P = 0.008).

Positive expression of HIF1a (score ≥ 1+) was associated with significantly greater DOI (Kruskal–Wallis test, P = 0.018), which means deep invading tumors. The expression of HIF1a alone did not correlate with SUV_{max}, MTV, or TLG (Kruskal–Wallis test, P = 0.184, P = 0.771, and P = 0.134, respectively).

CD44 expression was not associated with any metabolic parameter and/or DOI (Kruskal–Wallis test, P > 0.05, not shown).

Hypoxia Score for Enhanced Accuracy

To optimize the likelihood of tissue-based tumor hypoxia detection, we created a hypoxia score by combining the scores of the immunohistochemical staining for GLUT1 and the binarized HIF1a, both known to be upregulated under hypoxic conditions. As shown in **Figure 3**, for both SUV_{max} and DOI, the association showed a dose–response relationship: the higher the hypoxia score, the higher the SUV_{max} and the deeper the tumor infiltration (Kruskal–Wallis test, P = 0.037, and P = 0.008, respectively).

Impact of SUV_{max}, DOI, and Hypoxia-Related Protein Expression on Oncological Outcomes

There were 14 (14.3%) local recurrences in the cohort, whereas 16 (16.3%) patients had regional recurrence, and 14

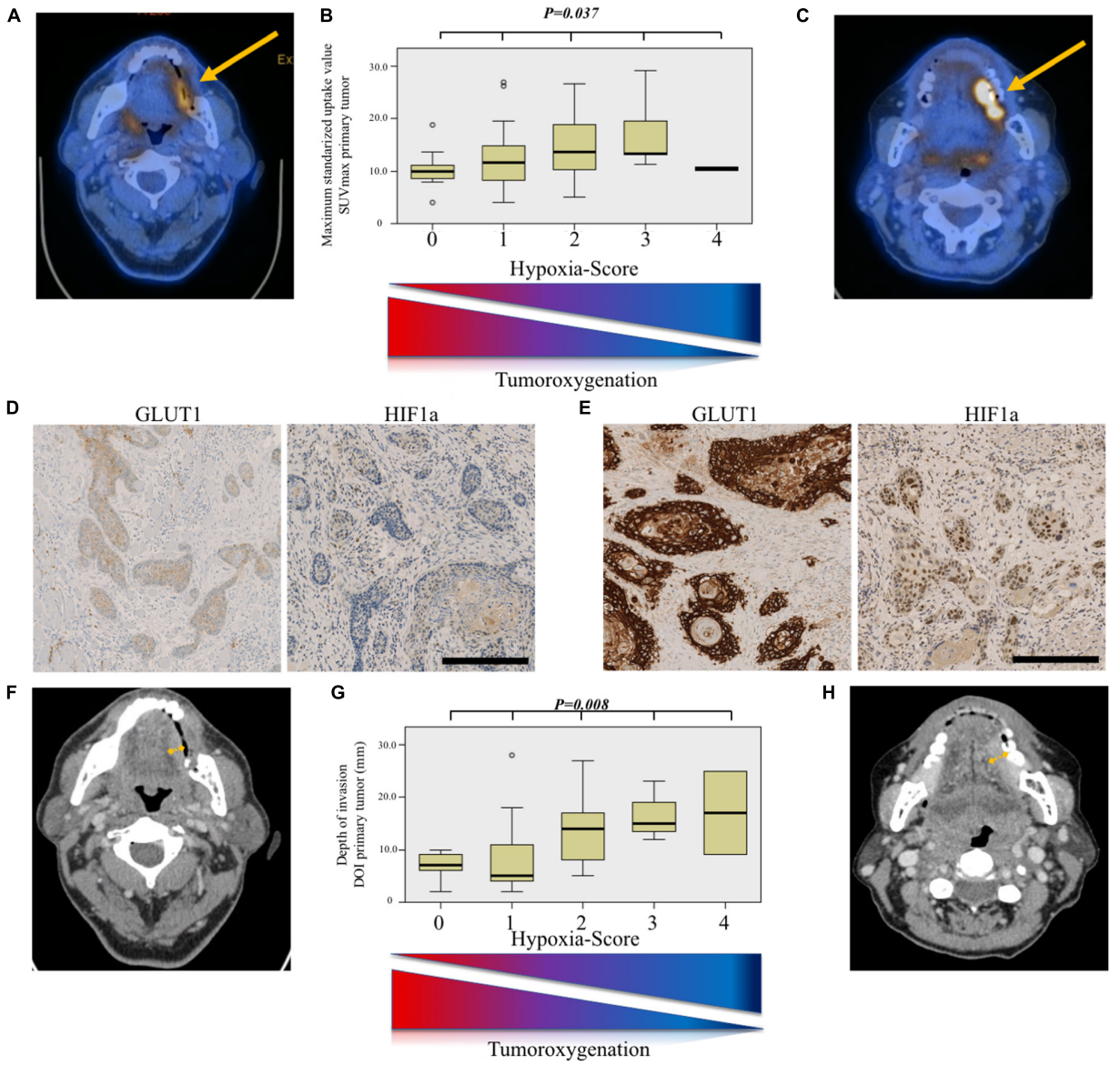

FIGURE 3 | Hypoxia-score model for prediction of aggressive tumor phenotype. **(A)** Axial 18-fluoro-desoxy-glucose positron emission tomography/computed tomography (FDG-PET/CT) image showing a weakly metabolically active tumor (SUV_{max} = 5.1). **(B)** Comparison of maximum standardized uptake value (SUV_{max}) value distribution according to hypoxia score. The higher the score, the higher the SUV_{max} (Kruskal–Wallis test, P = 0.037). **(C)** Axial FDG-PET/CT image showing a strongly metabolically active tumor (SUV_{max} = 19.4). **(D)** Immunohistochemical staining for glucose transporter 1 (GLUT1) and hypoxia-inducible factor 1-alpha (HIF1a) showing a weak membranous and nuclear staining, respectively, resulting in a low hypoxia score. Scale bar, 250 μm. **(E)** Immunohistochemical staining for GLUT1 and HIF1a showing a strong membranous and nuclear staining, respectively, resulting in a high hypoxia score. Scale bar, 250 μm. **(F)** Axial contrast-enhanced computed tomography (CT) image in the same patient as **(A)** showing a tumor with modest depth of invasion (DOI). Definitive DOI on histopathology was 2 mm. **(G)** Comparison of depth of invasion (DOI, mm) value distribution according to hypoxia score. The higher the score, the deeper the tumoral infiltration (Kruskal–Wallis test, P = 0.008). **(H)** Axial contrast-enhanced computed tomography (CT) image in the same patient as **(C)** showing a tumor with deeper invading tumor. Definitive DOI on histopathology was 6 mm.

(14.3%) had distant metastasis. Fifteen (15.3%) patients died from their tumor.

As shown in **Figure 4A**, local recurrence-free survival was significantly worse for patients with higher SUV_{max} of the primary tumor (log-rank test, P = 0.047). For regional recurrence-free, distant metastasis-free, and disease-specific survival, there was no statistically significant difference (log-rank test, P = 0.140, not shown; P = 0.131, **Figure 4B**; and P = 0.142, **Figure 4C**; respectively).

As shown in **Figures 4D–F**, local recurrence-free survival, distant metastasis-free, and disease-specific survival were significantly worse for patients with deep invading tumors (log-rank test, P = 0.033, **Figure 4D**; P = 0.045, **Figure 4E**; and P = 0.017, **Figure 4F**; respectively). There was no statistically

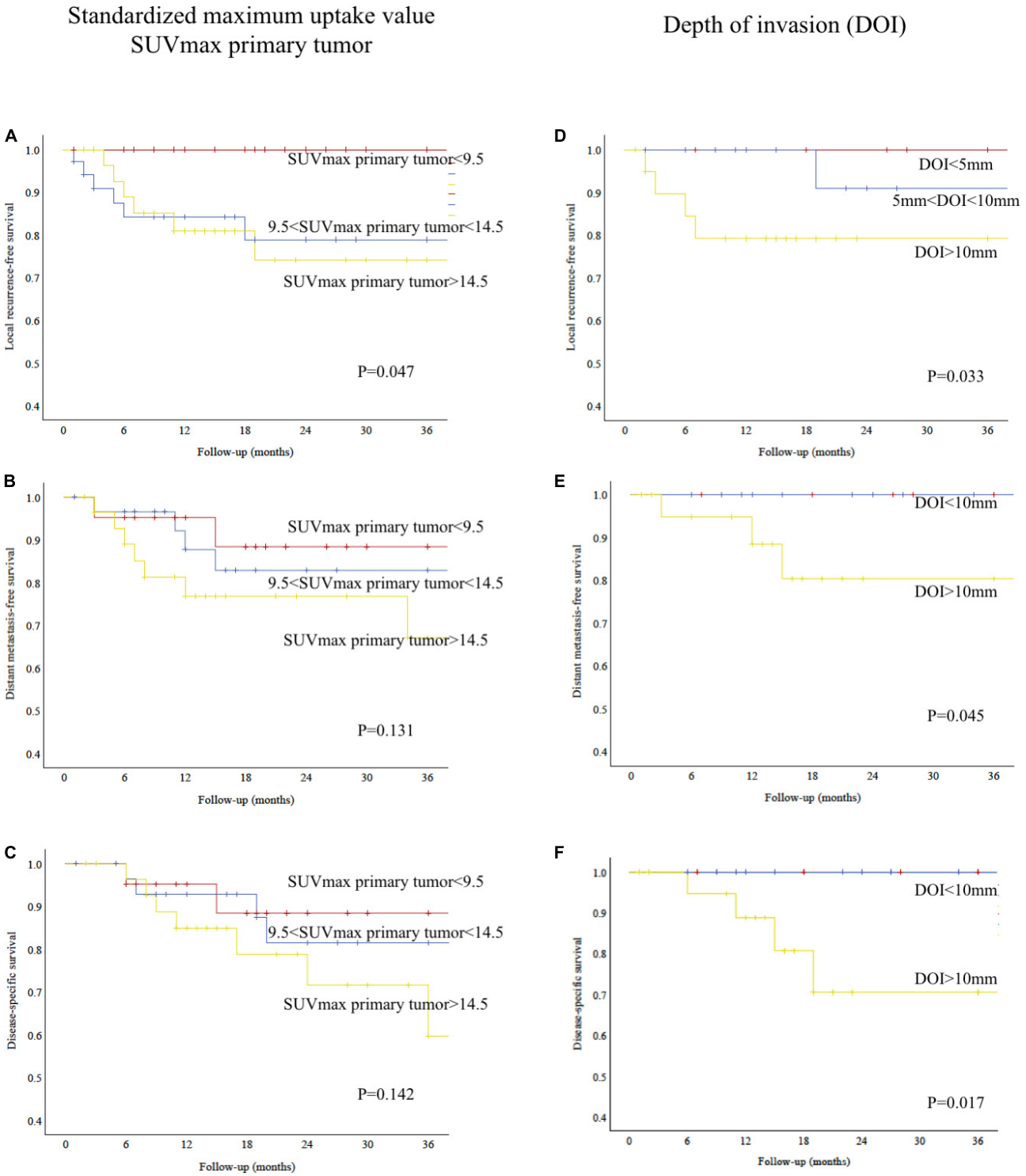

FIGURE 4 | (A) Kaplan–Meier analysis showing relative survival according to SUV_{max} of primary tumor. High SUV_{max} predicted poorer local recurrence-free survival (log-rank test, $P = 0.047$). **(B)** Kaplan–Meier analysis showing distant metastasis-free survival according to SUV_{max} of primary tumor (log-rank test, $P = 0.131$). **(C)** Kaplan–Meier analysis showing disease-specific survival according to SUV_{max} of primary tumor (log-rank test, $P = 0.142$). **(D)** Kaplan–Meier analysis showing relative survival according to depth of invasion (DOI). Patients with deep tumors had a poorer local recurrence-free survival (log-rank test, $P = 0.033$). **(E)** Kaplan–Meier analysis showing distant metastasis-free survival according to depth of invasion (DOI). Patients with deep tumors had a poorer distant metastasis-free survival (log-rank test, $P = 0.045$). **(F)** Kaplan–Meier analysis showing disease-specific survival according to depth of invasion (DOI). Patients with deep tumors had a poorer disease-specific survival (log-rank test, $P = 0.017$).

significant difference for regional recurrence-free survival (log-rank test, $P = 0.275$, not shown).

When directly correlating expression of GLUT1, HIF1a, and hypoxia score with oncological outcomes, patients showing a strong expression of GLUT1 (score > 2+) had a poorer local recurrence-free survival (log-rank test, $P = 0.050$, not shown). Similarly, patients with a high tissue-based hypoxia score (>3) had a poorer local recurrence-free survival (log-rank test, $P = 0.031$, not shown).

For regional recurrence-free, distant metastasis-free, and disease-specific survivals, expression of GLUT1, HIF1a, and hypoxia score did not predict survival (log-rank test, $P > 0.05$, not shown).

Multivariable Cox Regression Analysis of Oncological Outcomes

We finally performed a multivariable Cox regression analysis including all relevant factors listed in **Table 1**, the hypoxia score, and SUV_{max} of the primary tumor.

For local recurrence-free survival, positive nodal disease (pN + vs. pN0) and SUV_{max} of primary tumor were independent predictors of survival ($P = 0.036$ and $P = 0.046$, respectively). All other factors were not independent predictors ($P > 0.05$).

For regional recurrence-free survival, positive nodal disease (pN + vs. pN0) was the sole independent predictor of recurrence ($P = 0.014$). All other factors were not independent predictors ($P > 0.05$).

For distant metastasis-free survival, advanced T classification (pT3–T4 vs. pT2–T1) and positive nodal disease (pN + vs. pN0) were independent predictors ($P = 0.013$ and $P = 0.031$, respectively). All other factors were not independent predictors ($P > 0.05$).

For disease-specific survival, positive nodal disease (pN + vs. pN0) was also the sole independent predictor ($P = 0.034$). All other factors were not independent predictors ($P > 0.05$).

DISCUSSION

This study evaluates in a cohort of OSCC the correlation between preoperative FDG-PET and outcome through histometabolic tumor imaging of hypoxia. Our study provides some important insights in OSCC with analysis of clinical, histological, and functional nuclear medicine imaging data, therefore creating a histometabolic profile of OSCC.

A hypoxia-related protein overexpression correlated with a higher *in vivo* uptake of glucose, estimated by SUV_{max} on preoperative FDG-PET. This allowed us for definition of a hypoxia score, correlating with DOI of the tumor. This information impacted on local control and metastatic spread in OSCC. As shown in our multivariable analysis, nodal involvement is the most important prognostic factor in OSCC, including for local recurrence-free survival, in concordance with previous publications (26, 27). Therefore, prehistological estimation of tumor aggressiveness and nodal status is very important.

When FDG-PET was first added to the staging process in head and neck squamous cell carcinoma, it improved the nodal classification (28), provided a more accurate detection of distant metastasis (29) and synchronous primary tumors (30), and increased the detection rate of occult primaries (31). Furthermore, it is used to assess local (32) and regional (33) tumor response after chemoradiation. These studies mostly used FDG-PET to evaluate the presence or absence of metabolic activity in a binary manner.

In recent years, studies have examined the potential of quantification of functional nuclear medicine imaging data, using parameters such as maximum SUV_{max}, MTV, TLG, or further mathematically derived value such as textural index. Their role in predicting radio-oncological outcomes has now also been demonstrated (9, 34–38). However, a growing body of evidence shows that these data could also be used as a predictive tool for outcomes deemed to be surgical (39), such as occult lymph node metastasis (11), bone infiltration in OSCC (40), or organ preservation in laryngeal and hypopharyngeal cancer (41, 42). Our study reinforces and confirms the prognostic role of SUV_{max} as a surrogate marker for surgical outcomes. We showed that SUV_{max} was an independent predictor of local recurrence-free survival in multivariable analysis. Furthermore, SUV_{max} strongly correlated with DOI, which is a major staging variable, recently integrated into the last edition of the UICC Staging System (3).

A DOI > 10 mm represents a crucial cutoff point from the anatomical and biological points of view in oral tongue and floor of mouth tumors since it marks the passage from the intrinsic to the extrinsic musculature (43). As such, it was implemented by the 8th edition of TNM Staging of UICC as the marking point between early (pT1–2) and advanced disease (pT3–4) (3). The importance of DOI > 10 mm has been also underlined in the survival analyses in this study (**Figures 4D–F**).

According to our ROC analysis, a SUV_{max} of primary tumor < 9.5 was the optimal cutoff to largely rule out DOI > 10 mm. On the other hand, a SUV_{max} > 14.5 predicted DOI > 10 mm with a rather good specificity. These data could be of adjunctive value in the everyday clinical practice, considering that tumors with DOI > 10 mm require compartment tongue surgical approach (44, 45).

First described by Otto Warburg (8), the ability of tumor cells to survive in an hypoxic environment is gained by promoting a shift toward glycolytic reductive metabolism rather than oxygen-dependent Krebs cycle (oxidative metabolism). Through increased production of reactive oxygen species (ROS) stimulated by hypoxia, upregulation of one of the main activators of the Warburg effect, HIF1a, is promoted (46). This allows adaptation to hypoxia by increasing GLUT1 expression, glycolysis, and lactate production (47). This deregulation in cellular energetics is associated with an induction of EMT through downregulation of E-cadherin and upregulation of twist1 and vimentin (6, 48). Furthermore, an invasive phenotype is promoted through matrix metalloproteinase upregulation (7). Some data indicate that increased SUV_{max} is associated with increased tissue necrosis assessed by, e.g., cleaved caspase 3 staining (49), further supporting the idea of an association between hypoxia and increased SUV_{max} by FDG-PET.

Therefore, our results seem logical and corroborate the findings from previous studies in a larger cohort (18–21). In studies with 36 OSCC and 33 T2-oral tongue cancer patients, a correlation of the primary tumor's SUV_{max} with GLUT1 and HIF1a expression was found (18, 19). In the first study by Yamada et al. (18), a high SUV_{max} was associated with higher T classification but not nodal status. Correlation with DOI was not performed, which, at the time of their study, was not yet part of the TNM staging system (3, 18). The second study by Han et al. reported that SUV_{max} correlated with hypoxic status assessed by HIF1a and GLUT1 and was predictive of survival in OSCC (19). Interestingly, despite similar results, the data from all of the studies were based on expression analysis of different tissue specimen (biopsy, tissue microarray, and whole slide stainings of the resection specimen in the current study).

Some smaller studies in OSCC did not show any correlation between SUV_{max}, GLUT1, and HIF1a. Yokobori et al. showed in 27 early stage OSCCs a correlation between SUV_{max}, T stage, and microvessel density but not with GLUT1 (20). In a further study with 31 OSCC patients, SUV_{max} and GLUT1 did not show any correlation, although both of them were predictors of outcome (21).

In other head and neck tumor sites, there are some divergent data as well. In a cohort of oropharyngeal and hypopharyngeal cancer patients, a correlation between SUV_{max}, GLUT1, and HIF1a expression was found (38). However, in a further study done mostly in oropharyngeal cancer patients, high GLUT1 expression correlated with EGFR expression and p16 negative status but not with SUV_{max} of the primary tumor (50). In recurrent head and neck squamous cell carcinoma, GLUT1 expression was elevated but did not correlate with SUV_{max} of the primary tumor (51).

Our study has some drawbacks due its retrospective nature not allowing a definitive statement about clinical applicability and the lack of mechanistic demonstration. Furthermore, the low number of events may have led to a beta error in some analyses. Finally, future studies shall examine the correlation between FDG-PET-derived hypoxia estimation and classical hypoxia tracers such as 18F-fluoromisonidazole [(^{18}F)-FMISO]-PET, which was shown to predict therapeutic response in clinical studies (52–54). Initial prospective and dynamic data could thereby show an association of HIF1a expression and an increased (^{18}F)-FMISO tumor uptake, indicating hypoxic conditions in a cohort of head and neck squamous cell carcinoma (HNSCC). However, only two carcinomas from the oral cavity were included in this study (55). Another study with 15 HNSCC patients did not show any correlation between immunohistochemical markers (including GLUT1 and HIF1a), FDG-PET parameters, and (^{18}F)fluoroerythronitroimidazole [(^{18}F)FETNIM]-PET, another hypoxia/perfusion tracer (56).

In conclusion, a quantification of the FDG uptake under standardized conditions can be used as a surrogate for tumor aggressiveness, since it correlates with the Warburg effect, tumor hypoxia, EMT, and invasiveness. It allows for definition of a histometabolic profile, allowing prehistological prediction of DOI and nodal status, the latter being the most important prognostic factor in OSCC. This information may be useful in surgical planning, indication for adjuvant radiotherapy, approach to the neck, and patient counseling.

DATA AVAILABILITY STATEMENT

The datasets generated for this study can be obtained upon reasonable request by email to the corresponding author.

ETHICS STATEMENT

The studies involving human participants were reviewed and approved by Kantonale Ethikkommission Zürich. The patients/participants provided their written informed consent to participate in this study.

AUTHOR CONTRIBUTIONS

GM and NR formulated the basic study idea. GM conducted patients search. MH extracted the data related to nuclear imaging. NR and GM performed immunohistological staining and scoring. GM extracted the patient-related data, performed statistical analysis, built the figures, and wrote the first draft of the manuscript. MB, PS, MH, and NR edited and reviewed the manuscript. GM, MB, PS, MH, and NR have participated substantially to the study and approved the final version of the manuscript. All authors contributed to the article and approved the submitted version.

FUNDING

This study was funded by a 10'000 CHF Zurich Cancer League Grant, awarded on May 23rd, 2019.

REFERENCES

1. Shah JP, Gil Z. Current concepts in management of oral cancer–surgery. *Oral Oncol.* (2009) 45:394–401. doi: 10.1016/j.oraloncology.2008.05.017
2. Broglie MA, Haile SR, Stoeckli SJ. Long-term experience in sentinel node biopsy for early oral and oropharyngeal squamous cell carcinoma. *Ann Surg Oncol.* (2011) 18:2732. doi: 10.1245/s10434-011-1780-6
3. Lydiatt WM, Patel SG, O'Sullivan B, Brandwein MS, Ridge JA, Migliacci JC, et al. Head and neck cancers—major changes in the American Joint Committee on cancer eighth edition cancer staging manual. *CA Cancer J Clin.* (2017) 67:122–37. doi: 10.3322/caac.21389
4. Morand GB, Ikenberg K, Vital DG, Cardona I, Moch H, Stoeckli SJ, et al. Preoperative assessment of CD44—mediated depth of invasion as predictor of occult metastases in early oral squamous cell carcinoma. *Head Neck.* (2018) 41:950–8. doi: 10.1002/hed.25532

5. da Silva SD, Morand GB, Alobaid FA, Hier MP, Mlynarek AM, Alaoui-Jamali MA, et al. Epithelial-mesenchymal transition (EMT) markers have prognostic impact in multiple primary oral squamous cell carcinoma. *Clin Exp Metastas.* (2015) 32:55–63. doi: 10.1007/s10585-014-9690-1
6. Joseph JP, Harishankar M, Pillai AA, Devi A. Hypoxia induced EMT: a review on the mechanism of tumor progression and metastasis in OSCC. *Oral Oncol.* (2018) 80:23–32. doi: 10.1016/j.oraloncology.2018.03.004
7. Qiao B, Johnson NW, Gao J. Epithelial-mesenchymal transition in oral squamous cell carcinoma triggered by transforming growth factor-beta1 is Snail family-dependent and correlates with matrix metalloproteinase-2 and -9 expressions. *Int J Oncol.* (2010) 37:663–668. doi: 10.3892/ijo_00000715
8. Warburg O. On the origin of cancer cells. *Science (New York N Y).* (1956) 123:309–14. doi: 10.1126/science.123.3191.309
9. Halfpenny W, Hain SF, Biassoni L, Maisey MN, Sherman JA, McGurk M. FDG-PET. A possible prognostic factor in head and neck cancer. *Br J Cancer.* (2002) 86:512–6. doi: 10.1038/sj.bjc.6600114
10. Queiroz MA, Hüllner M, Kuhn F, Huber G, Meerwein C, Kollias S, et al. PET/MRI and PET/CT in follow-up of head and neck cancer patients. *Eur J Nuc Med Mol Imaging.* (2014) 41:1066–75. doi: 10.1007/s00259-014-2707-9
11. Morand GB, Vital DG, Kudura K, Werner J, Stoeckli SJ, Huber GF, et al. Maximum standardized uptake value (SUV max) of primary tumor predicts occult neck metastasis in oral cancer. *Sci Rep.* (2018) 8:11817. doi: 10.1038/s41598-018-30111-7
12. Peinado H, Cano A. A hypoxic twist in metastasis. *Nat Cell Biol.* (2008) 10:253–4. doi: 10.1038/ncb0308-253
13. Tam SY, Wu VWC, Law HKW. Hypoxia-induced epithelial-mesenchymal transition in cancers: HIF-1α and beyond. *Front Oncol.* (2020) 10:486. doi: 10.3389/fonc.2020.00486
14. Swartz JE, Pothen AJ, Stegeman I, Willems SM, Grolman W. Clinical implications of hypoxia biomarker expression in head and neck squamous cell carcinoma: a systematic review. *Cancer Med.* (2015) 4:1101–16. doi: 10.1002/cam4.460
15. Beasley NJ, Leek R, Alam M, Turley H, Cox GJ, Gatter K, et al. Hypoxia-inducible factors HIF-1α and HIF-2α in head and neck cancer: relationship to tumor biology and treatment outcome in surgically resected patients. *Cancer Res.* (2002) 62:2493–7.
16. Le Q-T, Kong C, Lavori PW, O'byrne K, Erler JT, Huang X, et al. Expression and prognostic significance of a panel of tissue hypoxia markers in head-and-neck squamous cell carcinomas. *Int J Radiat Oncol Biol Phys.* (2007) 69:167–75. doi: 10.1016/j.ijrobp.2007.01.071
17. Linge A, Lohaus F, Löck S, Nowak A, Gudziol V, Valentini C, et al. HPV status, cancer stem cell marker expression, hypoxia gene signatures and tumour volume identify good prognosis subgroups in patients with HNSCC after primary radiochemotherapy: a multicentre retrospective study of the German Cancer Consortium Radiation Oncology Group (DKTK-ROG). *Radiother Oncol.* (2016) 121:364–73. doi: 10.1016/j.radonc.2016.11.008
18. Yamada T, Uchida M, Kwang-Lee K, Kitamura N, Yoshimura T, Sasabe E, et al. Correlation of metabolism/hypoxia markers and fluorodeoxyglucose uptake in oral squamous cell carcinomas. *Oral Surgery Oral Med Oral Pathol Oral Radiol.* (2012) 113:464–71. doi: 10.1016/j.tripleo.2011.04.006
19. Han MW, Lee HJ, Cho KJ, Kim JS, Roh JL, Choi SH, et al. Role of FDG—PET as a biological marker for predicting the hypoxic status of tongue cancer. *Head Neck.* (2012) 34:1395–402.
20. Yokobori Y, Toyoda M, Sakakura K, Kaira K, Tsushima Y, Chikamatsu K. (18)F-FDG uptake on PET correlates with biological potential in early oral squamous cell carcinoma. *Acta Oto Laryngolo.* (2015) 135:494–9.
21. Kunkel M, Reichert TE, Benz P, Lehr HA, Jeong JH, Wieand S, et al. Overexpression of Glut-1 and increased glucose metabolism in tumors are associated with a poor prognosis in patients with oral squamous cell carcinoma. *Cancer.* (2003) 97:1015–24. doi: 10.1002/cncr.11159
22. Pfister DG, Spencer S, Brizel DM, Burtness B, Busse PM, Caudell JJ, et al. Head and neck cancers, Version 2.2014. Clinical practice guidelines in oncology. *J Natl Comprehens Cancer Netw.* (2014) 12:1454–87. doi: 10.6004/jnccn.2014.0142
23. Rupp NJ, Schüffler PJ, Zhong Q, Falkner F, Rechsteiner M, Rüschoff JH, et al. Oxygen supply maps for hypoxic microenvironment visualization in prostate cancer. *J Pathol Inform.* (2016) 7:3. doi: 10.4103/2153-3539.175376
24. Sekine T, Delso G, Zeimpekis KG, de Galiza Barbosa F, Ter Voert E, Huellner M, et al. Reduction of (18)F-FDG dose in clinical PET/MR imaging by using silicon photomultiplier detectors. *Radiology.* (2018) 286:249–59.
25. Nojima M, Tokunaga M, Nagamura F. Quantitative investigation of inappropriate regression model construction and the importance of medical statistics experts in observational medical research: a cross-sectional study. *BMJ Open.* (2018) 8:e021129. doi: 10.1136/bmjopen-2017-021129
26. Liao C-T, Chang JT-C, Wang H-M, Ng S-H, Hsueh C, Lee L-Y, et al. Analysis of risk factors of predictive local tumor control in oral cavity cancer. *Annal Surg Oncol.* (2008) 15:915–22. doi: 10.1245/s10434-007-9761-5
27. Tankéré F, Camproux A, Barry B, Guedon C, Depondt J, Gehanno P. Prognostic value of lymph node involvement in oral cancers: a study of 137 cases. *Laryngoscope.* (2000) 110:2061–5. doi: 10.1097/00005537-200012000-00016
28. Kyzas PA, Evangelou E, Denaxa-Kyza D, Ioannidis JP. 18F-fluorodeoxyglucose positron emission tomography to evaluate cervical node metastases in patients with head and neck squamous cell carcinoma: a meta-analysis. *J Natl Cancer Institute.* (2008) 100:712–20. doi: 10.1093/jnci/djn125
29. Haerle SK, Schmid DT, Ahmad N, Hany TF, Stoeckli SJ. The value of (18)F-FDG PET/CT for the detection of distant metastases in high-risk patients with head and neck squamous cell carcinoma. *Oral Oncol.* (2011) 47:653–9. doi: 10.1016/j.oraloncology.2011.05.011
30. Haerle SK, Strobel K, Hany TF, Sidler D, Stoeckli SJ. (18)F-FDG-PET/CT versus panendoscopy for the detection of synchronous second primary tumors in patients with head and neck squamous cell carcinoma. *Head Neck.* (2010) 32:319–25. doi: 10.1002/hed.21184
31. Miller FR, Hussey D, Beeram M, Eng T, McGuff HS, Otto RA. Positron emission tomography in the management of unknown primary head and neck carcinoma. *Arch Otolaryngol Head Neck Surgery.* (2005) 131:626–9. doi: 10.1001/archotol.131.7.626
32. Ong SC, Schoder H, Lee NY, Patel SG, Carlson D, Fury M, et al. Clinical utility of 18F-FDG PET/CT in assessing the neck after concurrent chemoradiotherapy for Locoregional advanced head and neck cancer. *J Nuc Med Off Pub Soc Nuc Med.* (2008) 49:532–40. doi: 10.2967/jnumed.107.044792
33. Mehanna H, Wong WL, McConkey CC, Rahman JK, Robinson M, Hartley AG, et al. PET-CT surveillance versus neck dissection in advanced head and neck cancer. *New Engl J Med.* (2016) 374:1444–54. doi: 10.1056/NEJMoa1514493
34. Higgins KA, Hoang JK, Roach MC, Chino J, Yoo DS, Turkington TG, et al. Analysis of pretreatment FDG-PET SUV parameters in head-and-neck cancer: tumor SUVmean has superior prognostic value. *Int J Radiat Oncol Biol Phys.* (2012) 82:548–53. doi: 10.1016/j.ijrobp.2010.11.050
35. Castelli J, De Bari B, Depeursinge A, Simon A, Devillers A, Roman Jimenez G, et al. Overview of the predictive value of quantitative 18 FDG PET in head and neck cancer treated with chemoradiotherapy. *Crit Rev Oncol Hematol.* (2016) 108:40–51. doi: 10.1016/j.critrevonc.2016.10.009
36. Allal AS, Dulguerov P, Allaoua MG, Haenggeli C-A, El-Ghazi EA, Lehmann W, et al. Standardized uptake value of 2-[(18) F] fluoro-2-deoxy-D-glucose in predicting outcome in head and neck carcinomas treated by radiotherapy with or without chemotherapy. *J Clin Oncol.* (2002) 20:1398–404. doi: 10.1200/JCO.2002.20.5.1398
37. Chen SW, Shen WC, Lin YC, Chen RY, Hsieh TC, Yen KY, et al. Correlation of pretreatment (18)F-FDG PET tumor textural features with gene expression in pharyngeal cancer and implications for radiotherapy-based treatment outcomes. *Eur J Nucl Med Mol Imaging.* (2017) 44:567–80. doi: 10.1007/s00259-016-3580-5
38. Lin YC, Chen RY, Chen SW, Hsieh TC, Yen KY, Liang JA, et al. Immunohistochemical studies and fluorodeoxyglucose uptake on positron emission tomography in pharyngeal cancer for predicting radiotherapy-based treatment outcomes. *Clin Otolaryngol.* (2017) 42:608–19. doi: 10.1111/coa.12783
39. Liao C-T, Chang JT-C, Wang H-M, Ng S-H, Hsueh C, Lee L-Y, et al. Pretreatment primary tumor SUVmax measured by FDG-PET and pathologic tumor depth predict for poor outcomes in patients with oral cavity squamous

cell carcinoma and pathologically positive lymph nodes. *Int J Radiat Oncol Biol Phys.* (2009) 73:764–71. doi: 10.1016/j.ijrobp.2008.05.004
40. Stalder SA, Schumann P, Lanzer M, Hüllner MW, Rupp NJ, Broglie MA, et al. Value of SUVmax for the prediction of bone invasion in oral squamous cell carcinoma. *Biology.* (2020) 9:23. doi: 10.3390/biology9020023
41. Werner J, Hullner MW, Rupp NJ, Huber AM, Broglie MA, Huber GF, et al. Predictive value of pretherapeutic maximum standardized uptake value (suvmax) in laryngeal and hypopharyngeal cancer. *Sci Rep.* (2019) 9:8972. doi: 10.1038/s41598-019-45462-y
42. Wichmann G, Kruger A, Boehm A, Kolb M, Hofer M, Fischer M, et al. Induction chemotherapy followed by radiotherapy for larynx preservation in advanced laryngeal and hypopharyngeal cancer: Outcome prediction after one cycle induction chemotherapy by a score based on clinical evaluation, computed tomography-based volumetry and (18)F-FDG-PET/CT. *Eur J Cancer (Oxford Engl).* (1990) 72:144–55. doi: 10.1016/j.ejca.2016.11.013
43. Piazza C, Montalto N, Paderno A, Taglietti V, Nicolai P. Is it time to incorporate 'depth of infiltration'in the T staging of oral tongue and floor of mouth cancer? *Curr Opin Otolaryngol Head Neck Surgery.* (2014) 22:81–9. doi: 10.1097/MOO.0000000000000038
44. Calabrese L, Bruschini R, Giugliano G, Ostuni A, Maffini F, Massaro MA, et al. Compartmental tongue surgery: long term oncologic results in the treatment of tongue cancer. *Oral Oncol.* (2011) 47:174–9. doi: 10.1016/j.oraloncology.2010.12.006
45. Piazza C, Grammatica A, Montalto N, Paderno A, Del Bon F, Nicolai P. Compartmental surgery for oral tongue and floor of the mouth cancer: oncologic outcomes. *Head Neck.* (2019) 41:110–5. doi: 10.1002/hed.25480
46. Calvo-Asensio I, Dillon ET, Lowndes NF, Ceredig R. The transcription factor Hif-1 enhances the radio-resistance of mouse MSCs. *Front Physiol.* (2018) 9:439. doi: 10.3389/fphys.2018.00439
47. Icard P, Shulman S, Farhat D, Steyaert JM, Alifano M, Lincet H. How the Warburg effect supports aggressiveness and drug resistance of cancer cells? *Drug Resist Updat.* (2018) 38:1–11. doi: 10.1016/j.drup.2018.03.001
48. Da Silva SD, Alaoui-Jamali MA, Soares FA, Carraro DM, Brentani HP, Hier M, et al. TWIST1 is a molecular marker for a poor prognosis in oral cancer and represents a potential therapeutic target. *Cancer.* (2014) 120:352–62. doi: 10.1002/cncr.28404
49. Deron P, Vangestel C, Goethals I, Potter A. De, Peeters M, Vermeersch H, et al. FDG uptake in primary squamous cell carcinoma of the head and neck. The relationship between overexpression of glucose transporters and hexokinases, tumour proliferation and apoptosis. Nuklearmedizin. *Nuc Med.* (2011) 50:15–21. doi: 10.3413/nukmed-0324-10-06
50. Baschnagel AM, Wobb JL, Dilworth JT, Williams L, Eskandari M, Wu D, et al. The association of (18)F-FDG PET and glucose metabolism biomarkers GLUT1 and HK2 in p16 positive and negative head and neck squamous cell carcinomas. *Radiother Oncol.* (2015) 117:118–24. doi: 10.1016/j.radonc.2015.08.025
51. Li SJ, Guo W, Ren GX, Huang G, Chen T, Song SL. Expression of Glut-1 in primary and recurrent head and neck squamous cell carcinomas, and compared with 2-[18F]fluoro-2-deoxy-D-glucose accumulation in positron emission tomography. *Br J Oral Maxillofac Surgery.* (2008) 46:180–6. doi: 10.1016/j.bjoms.2007.11.003
52. Grkovski M, Schoder H, Lee NY, Carlin SD, Beattie BJ, Riaz N, et al. Multiparametric imaging of tumor hypoxia and perfusion with (18)F-fluoromisonidazole dynamic PET in head and neck cancer. *J Nucl Med.* (2017) 58:1072–80. doi: 10.2967/jnumed.116.188649
53. Löck S, Perrin R, Seidlitz A, Bandurska-Luque A, Zschaeck S, Zöphel K, et al. Residual tumour hypoxia in head-and-neck cancer patients undergoing primary radiochemotherapy, final results of a prospective trial on repeat FMISO-PET imaging. *Radiother Oncol.* (2017) 124:533–40. doi: 10.1016/j.radonc.2017.08.010
54. Sato J, Kitagawa Y, Watanabe S, Okamoto S, Ohga N, Asaka T, et al. 18F-Fluoromisonidazole positron emission tomography (FMISO-PET) may better reflect hypoxia and cell proliferation activity in oral squamous cell carcinoma than 18F-fluoro-2-deoxyglucose (FDG)-PET: the third study. *J Nucl Med.* (2017) 58:284–284.
55. Nicolay NH, Wiedenmann N, Mix M, Weber WA, Werner M, Grosu AL, et al. Correlative analyses between tissue-based hypoxia biomarkers and hypoxia PET imaging in head and neck cancer patients during radiochemotherapy-results from a prospective trial. *Eur J Nucl Med Mol Imaging.* (2020) 47:1046–55. doi: 10.1007/s00259-019-04598-9
56. Grönroos TJ, Lehtiö K, Söderström KO, Kronqvist P, Laine J, Eskola O, et al. Hypoxia, blood flow and metabolism in squamous-cell carcinoma of the head and neck: correlations between multiple immunohistochemical parameters and PET. *BMC Cancer.* (2014) 14:876. doi: 10.1186/1471-2407-14-876

Conflict of Interest: MH is a recipient of grants from GE Healthcare and received an Alfred and Annemarie von Sick grant for translational and clinical cardiac and oncological research.

The remaining authors declare that the research was conducted in the absence of any commercial or financial relationships that could be construed as a potential conflict of interest.